International Journal of Information, Control and Computer Sciences
ISSN: 2517-9942
Vol:1, No:10, 2007

Evaluation of Graph-based Analysis for Forest Fire Detections

Young Gi Byun, Yong Huh, Kiyun Yu, Yong Il Kim

***Abstract*—** Spatial outliers in remotely sensed imageries represent observed quantities showing unusual values compared to their neighbor pixel values. There have been various methods to detect the spatial outliers based on spatial autocorrelations in statistics and data mining. These methods may be applied in detecting forest fire pixels in the MODIS imageries from NASA's AQUA satellite. This is because the forest fire detection can be referred to as finding spatial outliers using spatial variation of brightness temperature. This point is what distinguishes our approach from the traditional fire detection methods. In this paper, we propose a graph-based forest fire detection algorithm which is based on spatial outlier detection methods, and test the proposed algorithm to evaluate its applicability. For this the ordinary scatter plot and Moran's scatter plot were used. In order to evaluate the proposed algorithm, the results were compared with the MODIS fire product provided by the NASA MODIS Science Team, which showed the possibility of the proposed algorithm in detecting the fire pixels.

***Keywords*—** Spatial Outlier Detection, MODIS, Forest Fire

I. Introduction

SPATIAL outliers in remotely sensed imageries represent pixel values that are significantly different from their neighborhoods even though it is not a case in entire imagery scale [1], [2], [3]. Up to now, numerous kinds of spatial outlier detection algorithms have been developed in the fields of statistics and data mining.

A graph-based analysis is one of typical methods to define spatial outliers, which enables researchers to do visual analysis with 2-D graph based on ordinary scatter plot and Moran's scatter plot [2]. The ordinary scatter plot method utilizes a linear regression equation of attribute values of locations and means of their neighbor values to find spatial outliers [1], [3]. In comparison, Moran's scatter plot method uses correlations of attributive values of locations with its neighboring values and the entire data values (the total value?) [2], [4],[5],[6].

These methods may be applied in detecting the pixels indicating forest fire from the remotely sensed imageries. A breakout of forest fire in an area brings rapid change in brightness temperature of the corresponding pixels compared to its surroundings [7], [8]. Therefore, forest fire pixels can be treated as thermal anomaly in an image that represents land surface temperature [8].

With this point, forest fire detection becomes a process of finding spatial outliers which reflect local instability or extremity with respect to its neighboring pixel values. In this paper, we applied and tested the two aforementioned scatter plot methods for forest fire detection with MODIS (Moderate Resolution Imaging Spectro-radiometer) sensor imageries from the AQUA, a satellite developed and controlled by NASA.

Traditionally, there have been three kinds of forest fire detection methods in remote sensing; the spectral method, the spatial method and the temporal method. The spectral method uses simple thresholds for single- or multi-band data to identify fire pixels [9]. The spatial method uses statistical characteristics of a local area, an average and a standard deviation of pixel values surrounding a pixel. In this case, every pixel is transformed to z-score values and a predefined threshold is used [10]. Note that the spectral method basically adopts a fixed threshold, while the spatial method employs variable thresholds [9]. The temporal method uses temperature differences between remotely sensed imageries acquired at different times [11]. At any rate, all of these methods have been modified according to their specific purposes and test regions for improved accuracy. As a noticeable case, the MODIS Science Team developed the contextual fire detection algorithm for MODIS based on the spatial method [12]. They aimed at a globally and practically applicable algorithm that takes into account relatively many factors, such as cloud effect, sun glint effect, desert boundary effect and coastal false effect, in order to prevent false detection [10]. As a result, the MODIS contextual algorithm is expected to be more stable than others despite the fact that it often misses small fires [9].

As the above literature shows, the approach proposed in this paper is far from that using the traditional methods. In this study, we wanted to know whether the graph-based analysis could be applicable to forest fire detection. Here, the ordinary scatter plot and Moran's scatter plot method are to be employed. Consequently, in the following sections two scatter plot analyses are introduced along with the proposal and evaluation of a set of new algorithms based on these approaches. As for the

Manuscript received November 15, 2005. This work was supported in part by the Korea Institute of Science & Technology Evaluation and Planning

Young Gi Byun is with the Spatial Informatics and Systems Lab., Seoul National Univ., Seoul, South Korea(phone: 82-2-880-7371; fax: 82-2-889-0032; e-mail:kko071@snu.ac.kr).

Yong Huh is with the Spatial Informatics and Systems Lab., Seoul National Univ., Seoul, South Korea(phone: 82-2-880-7371; fax: 82-2-889-0032; e-mail:hy21262@dreamwiz.com).

Kiyun Yu is with the Spatial Informatics and Systems Lab., Seoul National Univ., Seoul, South Korea(phone: 82-2-880-7371; fax: 82-2-889-0032; e-mail:kiyun@snu.ac.kr).

Yong Il Kim is with the Spatial Informatics and Systems Lab., Seoul National Univ., Seoul, South Korea(phone: 82-2-880-7371; fax: 82-2-889-0032; e-mail:yik@plaza.snu.ac.kr).

test imagery, a MODIS satellite data covering the South Korean peninsula is used, and the evaluation is carried out by comparing the results from the product provided by the NASA MODIS Science Team for the same data.

II. Methodology

All objects above absolute zero (-273C or 0 K) emit radiant energy according to Plank's function which explains the radiant energy by means of the wavelength observed and the object's surface temperature [14]. Ideally, land surface temperatures of each band derived by inverse Plank's function should be the same. However, due to many factors, such as reflected solar radiation, surface emissivity differences and water vapor attenuation, there are some differences in temperature between bands. The differences are larger when one part of a pixel is substantially warmer than the rest [12]. The hotter the object is, the more contribution in radiance is observed in the shorter wavelengths than in their longer counterparts. As a result, in the case of a physically hot phenomenon like a forest fire, surface temperatures of both bands increase, in which the surface temperature of the shorter wavelength band is dramatically higher then that of the longer wavelength band. The level of increase is proportional to the magnitude of fire [7]. Traditionally, bands of near 4 μm and 11 μm wavelengths are used in forest fire detection. Here, the former represents the shorter wavelength while the latter represents the longer wavelength band [7], [9], [12].

A. Graph-based Fire Detection

A breakout of forest fire in an area brings different changes in brightness temperature in 4 μm and 11 μm wavelengths, respectively [9]. Once a forest fire breaks out, brightness temperature in 4 μm changes significantly compared to the changes in 11 μm [7]. Considering such a phenomenon, pixels that are suspected to indicate forest fire are selected. Subsequently, the corresponding brightness temperature in 4 μm (T_4) is used as a single spatial variable in the ordinary scatter plot and Moran's scatter plot. Detailed results of the proposed algorithms are described in the following paragraphs.

1) Ordinary Scatter Plot

The ordinary scatter plot shows the brightness temperature T4 on the X-axis and the average brightness temperature T4 in the surrounding area on the Y-axis (Figure 1(a)). A least square regression line is used to identify abnormal pixels. In this plot, the fire pixels are marked with red points that show significant standardized errors from the least square regression line [1]. Two points are found above the line and the other is below.

Assuming that errors are normally distributed, a standardized residual $s\varepsilon = \left|(\varepsilon - \mu_\varepsilon)/\sigma_\varepsilon\right| > \theta$ is a common test, in which μ_ε and σ_ε represent the mean and standard deviation of the distribution of the error term ε, respectively. Pixels with standardized residuals that are greater than θ or less than $-\theta$ are flagged as possible fire pixels. In figure 1 (a), points (a), (b) and (c) turn out to be the farthest from the regression line and thus have a high potential to be fire pixels. As a threshold, we let θ=3 to detect the final fire pixels in the ordinary scatter plot method.

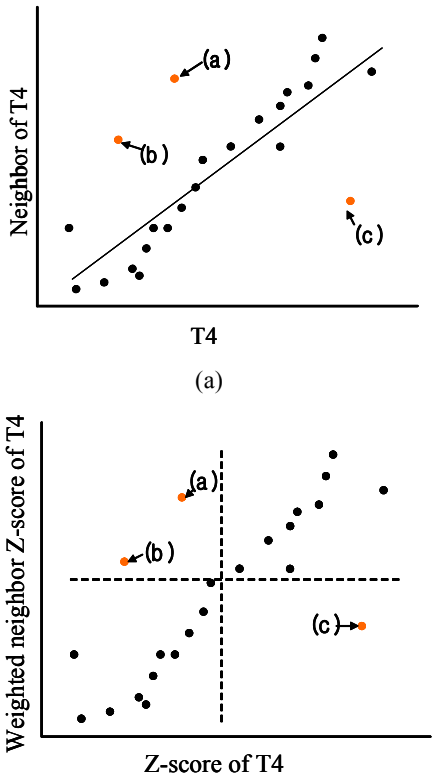

Fig. 1 Ordinary scatter plot(a) and Moran's scatter plot(b)

2) Moran's Scatter Plot

Moran's I is a simple translation of a non-spatial correlation measure into a spatial context and is one of the oldest indicators of spatial autocorrelation. Spatial autocorrelation is based on the first law of geography: near things are more similar than are more distant [5]. Positive spatial autocorrelation is yielded when neighboring areas are similar or the same. The Moran statistics can measure both the global trend and the local trend of data set. The global Moran's I measures global spatial autocorrelation of a data set while local Moran's I measures local spatial autocorrelation of a data set. The global Moran's I is defined as

$$I = \frac{n}{\sum_i^n \sum_j^n w_{ij}} \frac{\sum_i^n \sum_j^n w_{ij}(x_i - \bar{x})(x_j - \bar{x})}{\sum_i^n (x_i - \bar{x})^2} \quad (1)$$

Where, *n* indicates a total data count, $\bar{x}$ the mean of total data,

x the spatial variable (T_4), and w_{ij} the element of spatial weight matrix. By dividing the numerator and denominator of equation (1) with n^2, and using row-standardized spatial weight matrix, the global Moran's I can be expressed in Z statistics as in equation (2).

$$I = \frac{n}{\sum_i^n \sum_j^n w_{ij}} \frac{\sum_i^n \sum_j^n w_{ij}(x_i - \bar{x})(x_j - \bar{x})}{\sum_i^n (x_i - \bar{x})^2} = \frac{1}{n} Z^T \tilde{Z} \quad (2)$$

In this study, we let w_{ij}=1 if pixel *i* and pixel *j* were adjacent to each other; otherwise w_{ij}= 0. Therefore, W is an adjacency matrix for the observed region.

The local Moran's I decomposes the global Moran's I into contribution of each location. Therefore, the local Moran's I can be used to identify fire pixels [6]. The local Moran's I for an observation of *i* may be defined as

$$I_i = z_i \times \sum_j^n w_{ij} z_j \quad (3)$$

where the observations z_i, z_j are in deviations from the mean, and the w_{ij} is an element from a spatial weights matrix W.

The Moran's scatter plot is a plot of normalized brightness temperature value against the neighborhood of normalized brightness temperature value ($W \cdot Z$) [6]. Where, W is the row-standardized spatial weight matrix. The row-standardized spatial weight matrix is created through the process of dividing the each element in the weight matrix by its row sum. The Moran's scatter plot contains four quadrants. The upper left and lower right quadrants of figure 1(b) indicate a spatial association of dissimilar values. Spatial outliers can be identified form theses two quadrants. However, in this paper we decided that pixels such as point (c), which is surrounded by low value neighbors in Moran's scatter plot, are final fire pixels because forest fire areas have a higher brightness temperature than their neighbors.

TABLE I
DIFFERENCE FUNCTION AND STATISTICAL TEST FUNCTION MODEL OF THIS STUDY

Model Building		
Method	Ordinary scatter plot	Moran's scatter plot
Difference function	$\varepsilon = E(x) - (m \times f(x) + b)$	$Z_i = \frac{f(x) - \mu_f}{\sigma_f}$ $I_i = \sum_j W_{ij} Z_j$
Statistical test function	$\left\| \frac{\varepsilon - \mu_\varepsilon}{\sigma_\varepsilon} \right\| > \theta$	*lower right qudrants*
Aggregate function	$\mu_\varepsilon, \sigma_\varepsilon, m, b$	μ_f, σ_f

III. IMPLEMENTATION DETAILS OF ALGORITHM

We thus propose new graph-based fire detection algorithms based on the aforementioned characteristics of forest fire pixels in surface temperature images. Figure 2 presents a flowchart of this study, which can be divided into three parts, a preprocessing of MODIS L1B data, an implementation of the forest fire detection algorithm, and an evaluation of the proposed algorithm.

The pre-processing is composed of a geometric correction, subset extraction of study area, and transformation of data from a radiance unit to temperature unit. We used ENVI 3.5, a satellite image processing software for the pre-processing.

To derive temperatures of each band, offset and scale data from a metadata of MODIS L1B data set is used to convert the digital number (DN) of the sensor measurements to spectral radiance measured by satellite sensors.

Generally, a surface temperature is derived by integrating the product of Planck's function and the relative spectral response function of a sensor within a bandwidth [7]. However, for the sake of convenience, we utilized a simple surface temperature estimation equation developed by CIMSS (Cooperative Institute for Meteorological Satellite Studies) of Wisconsin University, which provides an effective central wavelength and a slope and offset for temperature estimation according to each MODIS band.

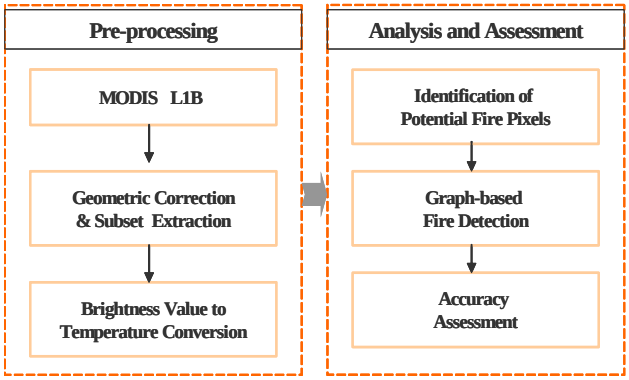

Fig. 2 Workflow of the study

Next, we performed a potential fire pixel test to reduce the execution time of the algorithm and to make the detection process more effective. This is done by removing obviously non-fire pixels such as clouds pixels or cold land pixels and identifying potential fire pixel which is probable to be real forest fire pixels. Then we applied the proposed fire detection algorithms to the potential fire pixels.

The non-fire pixels, such as cloud or water body pixels can cause serious problem in the contextual fire detection [15]. Thus, detections and removals of such pixels are important and necessary in the preprocessing. However, it is very difficult to identify exact cloud pixels because there exist not only thick clouds but also thin clouds as well.

In general, clouds have low radiance value in 4 μm and 12 μm band compared to land surface. From this we can detect

cloud pixels. In this study, we identified potential fire pixels using two criteria:

$$Criterion1: R_4 > \max(\overline{R}_4, \overline{R}_{4w}) \quad and \quad R_{12} > \max(\overline{R}_{12}, \overline{R}_{12w})$$
$$Criterion2: \nabla T = (T_{12} - T_4) > 8K \tag{4}$$

Here, R_4, R_{12} indicate radiance of 4 μm and 12 μm bands, respectively. On the other hand, $\overline{R}_4, \overline{R}_{12}$ indicate mean radiance of 4 μm and 12 μm bands in full image, respectively, whereas $\overline{R}_{4W}, \overline{R}_{12W}$ indicate mean radiance of 4 μm and 12 μm bands in local window. Such simple criteria can screen out more than half of the pixels to be processed and eliminate cloud and sun glint pixels [8].

Finally, we calculated the user accuracy and producer accuracy of the proposed algorithms by comparing their detection results with the ground data provided by the Korea Forest Service(KFS)[17]. KFS has built a forest fire database in terms of igniting and extinguishing times, locations, burnt areas, and other related information. Subsequently, the performance of the algorithms is evaluated through the comparison of the resulting accuracy with that of the MODIS fire product provided by the NASA MODIS Science Team.

IV. Study Area and Materials

The MODIS L1B data used in this paper is a set of imageries covering the South Korean peninsula taken by NASA's AQUA satellite. A metadata of these imageries is shown in Table 2. We used five imageries taken on April 5th and 11th of 2005, February 9th and 14th of 2004, and April 2nd of 2003.

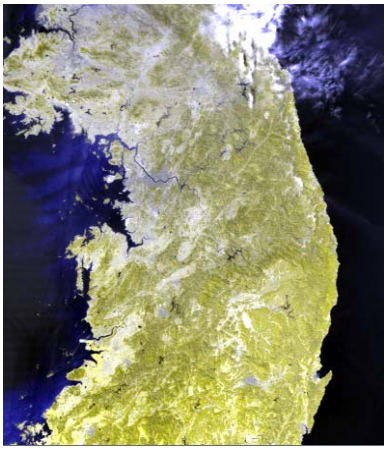

Fig. 3 MODIS RGB image of South Korea peninsula

TABLE 2
METADATA OF IMAGERIES USED

Satellite Name	AQUA
Sensor Used	MODIS
Spatial Resolution	1km
Number of Band	36
Area Covered	South Korea
Date of Acquisition	2003.04, 2004.02 2005.04

The MODIS bands used in our study are listed in Table 3. In detecting forest fire from the MODIS imagery, band 21 as well as band 22 was used to solve the problem of sensor saturation. The above-mentioned two bands have the same band width. Sensor saturation takes place when radiance that reaches the sensor is beyond the upper limit of the sensor's sensing range [12]. Radiance subject to sensor saturation is recorded as the upper limit of the sensing range.

In other words, all radiances higher than the upper limit of the sensing range are recorded as the upper limit. As a result, when radiance is higher than the upper limit, accurate radiance can not be identified. In band 22 sensor saturation takes place when brightness temperature is over 330K, and in band 21 it takes place when it is over 550K [12]. Therefore, the problem of sensor saturation was solved by using band 21 when sensor saturation took place in band 22.

TABLE 3
SPECIFICATIONS OF BAND FOR FIRE DETECTION

Band number	Bandwidth(μm)
21	3.930-3.989
22	3.930-3.989
31	10.780-11.280
32	11.770-12.270

Reference data for accuracy assessment was provided by the Korea Forest Service forest fire information system. The KFS data included the original location of forest fires, the time of breakout and extinction, the size of damaged areas, and the cause of forest fires. In making use of the data, it was troublesome because the data was not referenced to geographic coordinates but addresses. Considering the spatial resolution of MODIS (1km on ground), we expected that there would be little possibility of misclassification from converting the addresses to approximate geographic coordinates. Thus, it was done as such. Regarding the time of image acquisition, the AQUA satellite scans Korea at around 13:30pm that forest fires that were running through this time was recorded. The size of damage area recorded in the KFS data can be tens to hundreds times as large as that of burnt area. Theoretically, MODIS can sense the forest fire with the temperature over at least 800~1000K and the area over 0.01ha (100m^2), and the detection accuracy is about 50% [10]. Therefore, the forest fire recorded in Korea Forest Service data was selected only when the size of damaged area was over 0.1ha.

V. Result and Analysis

In this paper, in addition to the accuracy assessment ,i.e. user accuracy and producer accuracy calculation, we compared the results with the one from the product provided by the NASA MODIS Science Team to examine applicability of the algorithm. The NASA team used the contextual algorithm to detect thermal anomalies, such as forest fires or volcanic eruptions [10], [16].

The contextual algorithm uses statistical analysis of surface temperatures in a local window centered on a pixel, in which discrimination is carried out in order to find out whether or not it is a fire pixel [10]. Instead of using fixed thresholds for determining fire pixels, the algorithm computes a mean and standard deviation of the temperature in a local window, and then thresholds are determined using equations as follow:

$$T_4 \geq \mu_4 + \alpha\,\sigma_4$$
$$T_{4-11} \geq \mu_{4-11} + \beta\,\sigma_{4-11} \quad (5)$$

Here, T_4 is the surface temperature of observing bands near 4 μm and T_{4-11} is temperature difference between 4 μm and 11 μm of a local window. μ_4 and μ_{4-11} are means of T_4 and T_{4-11}, σ_4 and σ_{4-11} are standard deviations of T_4 and T_{4-11}, respectively, and α and β are constant values.

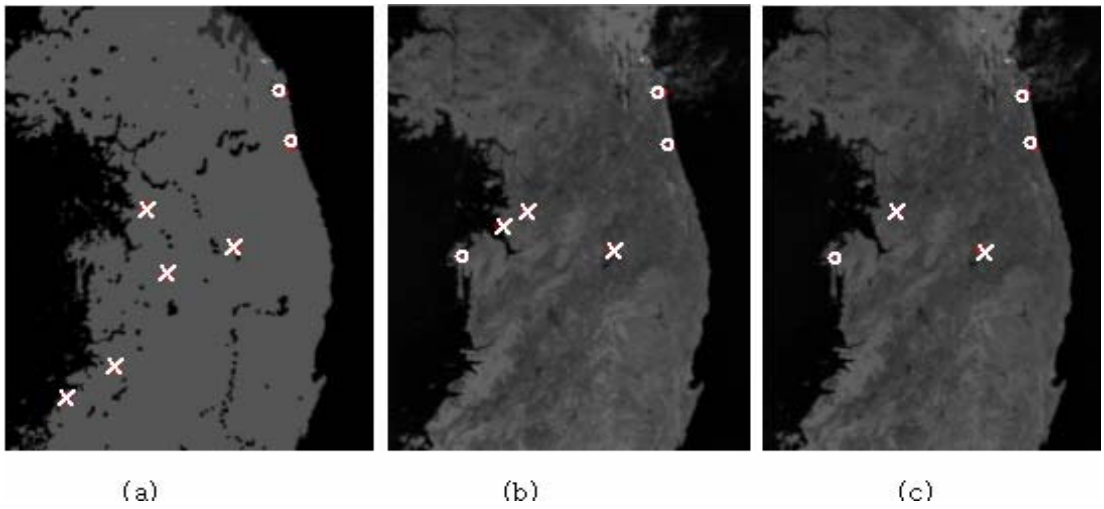

Fig. 4 Detection results using ordinary scatter plot(a), Moran's scatter plot(b), MODIS fire product(c)

Thus, the proposed fire detection algorithms were applied on the imageries and accuracies were assessed by checking the classified fire pixels against the data from the Korea Forest Service. To understand mechanisms between the commission and omission error, both the producer accuracy and user accuracy were calculated. Then, the same imageries were used by the method provided by the NASA MODIS Science Team and both the producer and user accuracy is calculated. The test results are shown in Table 4.

TABLE 4
ACCURACY TEST RESULTS

	Ordinary Scatter Plot	**Moran's Scatter Plot**	**MODIS Fire Product**
Total Number of Detected Fire Pixels	25	40	35
Number of True Fire Pixels in Detected Pixels	12	15	11
Number of Omission Error	14	11	15
Number of Commission Error	13	25	24
Producer Accuracy(%)	48	37.5	31.42
User Accuracy(%)	46.15	57.6	42.3

As shown in Table 4, the proposed algorithm based on the ordinary scatter plot showed a producer accuracy which was about 16% higher than that of the MODIS fire project. On the other hand, the user accuracy turned out to be 3% higher than that of the MODIS fire product. A similar trend appears in Moran's scatter plot case; about 6% higher in producer accuracy and about 15% higher in user accuracy than that of the MODIS fire product.

The ordinary scatter plot fire detection did not improve user accuracy considerably, whereas it reduced the commission error significantly compared to the MODIS fire product. In contrast, the Moran's scatter plot fire detection had high user accuracy with relatively high commission error. Such results were partly due to the incineration plant and the dense industrial area. These areas were misclassified as forest fires and such misclassifications were included in the commission error.

Moreover, the ordinary scatter plot algorithm was problematic in that large forest fires with extremely high temperatures were so influential in OLS (Ordinary Least Square) estimation that they made it difficult to detect small forest fires. On the other hand, Moran's scatter plot algorithm showed the problem of not considering the amount of relative spatial variation because it detected forest fire pixels based only on the location of the pixel in Moran's scatter plot

without numerical consideration.

From the above results, the proposed algorithms are considered as applicable in detecting forest fire pixels for they yielded higher accuracies as the MODIS fire product. An advantage of this approach is of use because it removes the step for determining complicated thresholds as in the traditional methods.

VI. Conclusion

This paper proposed graph-based forest fire detection algorithms which detect forest fire pixels in MODIS L1B imagery. The algorithm used spatial statistics reflecting spatial variation. After applying and testing the algorithms, the following results are acquired.

The algorithms yielded higher user and producer accuracies than those of the MODIS fire product provided by the NASA MODIS Science Team. Such a result does not mean that the proposed algorithms work better than the traditional fire detection methods developed so far. Rather, it implies the proposed algorithms have potentials to be applied in detecting the fire pixels and thus we need to put more intention on it. Looking at the algorithms, they are easy to use because they do not need the step for determining the threshold empirically according to the target regions. Thus, the algorithms have advantages over the traditional methods.

From the test, the ordinary scatter plot algorithm was proven problematic in that it was not sensitive to small forest fires, while Moran's scatter plot was also weak for it entailed a more and less high commission error due to the absence of a numerical criterion for spatial variation.

Thus, future research may put its focus on relieving such problems. One idea is in introducing spatial weight matrices that reflects the spatial variation of forest fire to decrease the commission error.

References

[1] S. Shekhar, C.T. Lu, and P. Zhang. "A unified approach to detecting spatial outliers," GeoInformatica, Vol.7, No.2, 2003, pp.139-166.

[2] S. Shekhar, C.T. Lu, and P. Zhang. "Detecting graph-based spatial outliers: algorithms and application(a summary of results)." *In Proc. the ACM SIGKDD international conference on Knowledge discovery and data mining*, , San Francisco, CA, USA , 2001, pp. 371-376.

[3] V.Barnett and T.Lewis, *Outliers in Statistical Data. 3rd edition*, John Wiley: New York, 1994.

[4] A.S.Forheringham, C.Brunsdon and M.Chatlton, *Quantitative Geography : Perspectives on Spatial Data Analysis*, London, UK: SAGE Publications, 2000, pp. 203-211.

[5] R. Haining, *Spatial Data Analysis : Theory and Practice*, Cambridge, UK: Cambridge Univ. Press, 2003, pp. 242-243.

[6] D, O'Sullivan and D.J.Unwin, Geographic Information Analysis, Hoboken, New Jersey: John Wiley & Sons, Inc., 2003, pp.196-201.

[7] J.Dozier, "A method for satellite identification of surface temperature fields of subpixel resolution," *Remote Sensing of Environment*, Vol.11, 1981, pp. 221–229.

[8] Ying Li, V. Anthony, R.L.Kremens, O. Ambrose and T. Chunqiang , "A Hybrid Contextual Approach to Wildland Fire Detection Using Multispectral Imagery," *IEEE Tran. Geoscience and remote sensing*, vol.43, No.9 September, 2005, pp. 2115-2126.

[9] Z. Li, Y.J.Kaufman, C.Ichoku, R.Fraser, A.Trishchenko, L.Giglio, J.Jin and X.Yu. (2000, Sep.), *A Review of AVHRR-based Active Fire Detection Algorithms: Principles, Limitations, and Recommendations*, Available : http://www.fao.org/gtos/gofc-gold/other.html

[10] L.Giglio, J.Descloitresa, C.O.Justicec and Y.J.Kaufman, "An Enhanced Contextual Fire Detection Algorithm for MODIS," *Remote Sensing of Environment*, vol. 87, 2003, pp. 273-282.

[11] R. LASAPONARA, V. CUOMO, M.F. MACCHIATO and T. SIMONIELLO, "A self-adaptive algorithm based on AVHRR multitemporal data analysis for small active fire detection," *INT.J. Remote Sensing*, Vol.24, No.8, 2003, pp.1723–1749.

[12] MODIS Science Team. (1998, Nov., 10), *Algorithm Technical Background Document ver2.2* Available: http://modis.gsfc.nasa.gov/data/atbd/atbd_mod14.pdf

[13] L.Giglioa, J.Descloitresa, C.O.Justicec and Y.J.Kaufman, "Evaluation of global fire detection algorithms using simulated AVHRR infrared data" *International journal of Remote Sensing*, 1998.

[14] J.R. Jensen Remote sensing of the environment : An earth resource perspective, Upper Saddle River, New Jersey: Prentice Hall, 2000, pp. 243-284.

[15] C.A.Seielstad, J.P.Riddering, S.R.Brown, L.P.Queen, and W.M.Hao, "Testing the Sensitivity of a MODIS-Like Daytime Active Fire Detection Model in Alaska Using NOAA/AVHRR Infrared Data," *Photogrammetric Engineering & Remote Sensing*, Vol.68, No.8, 2002, pp.831-838.

[16] C.O.Justice, L. Giglio, S. Korontzi, J. Owens, J.T. Morisette, D. Roy, J. Descloitres, S. Alleaume,F. Petitcolin and Y. Kaufman, "The MODIS fire products," *Remote Sensing of Environment*, Vol. 83, 2002, pp. 244–262.

[17] Korea Forest Service http://www.foa.go.kr/

Young Gi Byun received the BS degree in mineral and energy resources engineering from Chonnam National University and MS degree in Remote Sensing from Seoul National University in South Korea in 2004. He is now a doctoral course in Seoul National University in Korea. He is now working on forest fire detection and mapping using RS techniques. His research interests lie in the area of image matching, pattern recognition, and image processing.

Yong Huh received the BS degree in civil, urban & geosystem engineering from Seoul National University in South Korea in 2001. He is now a doctoral course in Seoul National University. He is now working on forest fire detection and mapping using RS techniques. His research interests lie in the area of digital image processing, pattern classification.

Kiyun Yu received the BS degree in civil engineering from Yonsei University in South Korea and PhD degree in GIS from University of Wisconsin-Madison in 1998. He was a director in the Ministry of Construction and Transportation until 2000. He is now an Assistant Professor of the School of Civil, Urban & Geosystem Engineering, Seoul National University in Korea.

Yong IL Kim received the BS degree and the PhD degree in Remote Sensing form Seoul National University in South Korea in 1988 and 1991, respectively. He is now an Associate Professor of the School of Civil, Urban & Geosystem Engineering, Seoul National University in Korea.